

Characteristic Wake Data for Local Blade Propeller Stalling

Jean Rebont,* Christian Maresca,† and Daniel Favier‡
Institute de Mechanique des Fluides de Marseille, Marseille, France

The aim of this experimental program is to show some effects of local blade stalling on the wake structure. The measurement of all the mean velocity components were carried out in the near wake of a four-bladed propeller, by use of a hot-film anemometric probe. In order to observe evolution of the wake structure, four values of the advance ratio γ are investigated. The two lower values of γ correspond to the stalled working conditions of the propeller, and the two upper values are in the vicinity of the maximum propeller efficiency. Some quantitative information about the stall characteristics was obtained from the velocity measurements. The flow separation in the stalled region of the blade decreases both the axial and radial velocity components, and increases the rotational speed of the wake. Furthermore, it was found that the stalled region first affected the blade tip and then grew from the tip towards the hub with decreasing values of γ .

Introduction

IN order to improve the understanding of the complex propeller problem, recent methods^{1,2} have used more accurate analytical simulation methods of wake models. Several of these methods define the complete wake geometry and have been based on theoretical models requiring few, but necessary, wake stability assumptions. Thus, by using high-speed computers, significant progress has been made towards a well-constructed wake model which applies to lower or mean rotor thrust levels. As propellers are pushed to greater thrust levels, wake distortion appears and can increase owing to the fact that stalling conditions may be reached. In such cases, the wake characteristics depart significantly from classical concepts of wake structures, and empirical investigations are required to improve the calculation assumptions of the theoretical wake model. In most cases, these empirical data are obtained from visualization tests (more often smoke techniques) which provide only qualitative information.

The practical drawbacks encountered when making measurements on the surface of a rotating airfoil, via such diagnostics as pressure transducers, are generally due, on the one hand, to the lack of space offered to the investigator in which to embed the measuring transducers without diminishing the blade structure, and on the other hand, to the centrifugal effect created by the blade rotation. Thus, flow analyses through the rotor are more and more carried out with the use of a fixed detector which is set up as closely as possible below the rotating plane. The high-frequency response of the detector permits the instantaneous observation of the phenomenon. The object of the present investigation is to obtain quantitative data for the high propeller loading. The three velocity components have been measured in the near wake of a four-bladed propeller for several values of the advance ratio, $\gamma = V_\infty / 2nR$ (where n is the rotation frequency, R the radius of the propeller, and V_∞ the freestream velocity). Two values of γ have been chosen so that the rotor operates at a high thrust coefficient τ ($\tau = T/\rho n^2 D^4$), where T is the thrust, ρ the density of air, and D the diameter of the propeller. The local blade stalling will be characterized through the subsequent analysis of the velocity profiles obtained for values of γ yielding large τ . The change of sign of the gradient of the thrust coefficient plotted vs γ (see Ref. 3) is

the criterion usually given to characterize global stalling. In Fig. 1, the experimental values τ , the power coefficient χ ($\chi = P/\rho n^3 D^5$, where P is the rotor power), and the efficiency coefficient η ($\eta = \gamma \tau / \chi$) of the four-bladed propeller described in Ref. 4, are plotted vs γ . The blade planform and the twist distribution can be deduced from Table 1. It is of interest to note that the τ curve has a maximum value for $\gamma = 0.48$, and a marked decrease for $\gamma < 0.48$. As had been noticed before,³ this decrease characterizes a flow separation on the blades. The purpose of this note is to analyze the effects of this flow separation on the velocity profiles measured in the blade wake.

Experimental Results and Discussion

The four-bladed propeller was tested in the open test section of the I.M.F.M. subsonic wind tunnel. The elliptical cross section ($3.3 \times 2.2 \text{ m}^2$) of that test section is 2.5 m long. The velocity was measured in the near-blade wake ($0.2 R$ downstream of the rotating plane, with $R = 0.425 \text{ m}$). The mean velocity components were determined according to the measurement method of waveform averaging, detailed in Refs. 4 and 5. To determine mean velocity, averages extended over 2000 revolutions. For 90° of propeller motion 100 azimuthal data points have been stored and averaged to compute the mean velocity. The formula for averages is given by

$$U = \frac{\int_{t=0}^{t=2000/n} \int_{\psi=0^\circ}^{\psi=90^\circ} u(t, \psi) d\psi dt}{\int_0^{2000/n} dt \int_{0^\circ}^{90^\circ} d\psi}$$

where ψ = azimuthal angle (Fig. 2), and t = time. The determination of the three velocity components results from an indirect method based on sums and differences of voltages recorded by a "V"-wedge-shaped hot-film detector (DISA 55 A 88), when the latter operates in four different directions (see Refs. 4 and 5), and leads to an absolute error of $\pm 0.02 \text{ m/sec}$ on any one of the three mean velocity components. The probe displacement along the blade radius, $\xi = r/R$, was obtained by an apparatus of teledriven gears. Voltages delivered by the hot film were then amplified and filtered through an intermediary electronic circuit, and finally mapped on an X-Y plotter whose X-scanning was synchronized with the probe displacement along the blade radius. This measurement technique finally permitted the determination of the mean components (tangential u , radial v , and axial w) defined in Fig. 2. Four values of the advance ratio γ have been selected: two lower values $\gamma = 0.37$ and 0.46 , corresponding to the

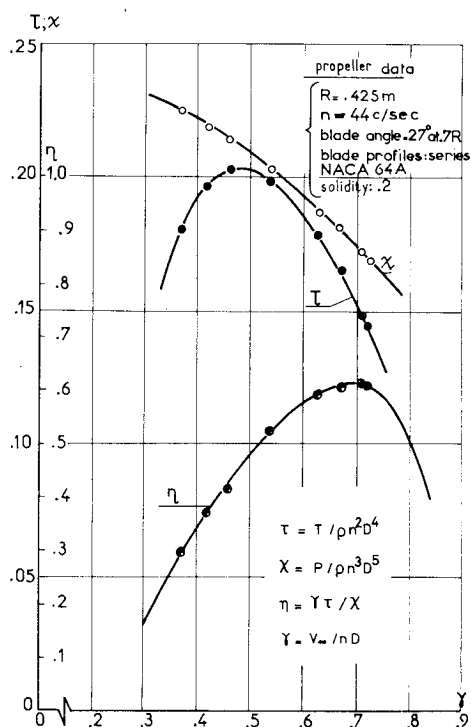
Received Dec. 13, 1974; revision received June 18, 1976.

Index category: Rotary Wing Aerodynamics.

*Ingenieur-Docteur au C.N.R.S.

†Charge de Recherche au C.N.R.S.

‡Attache de Recherche au C.N.R.S.

Fig. 1 Variation of coefficients τ , χ , η vs γ .

stalled working conditions (see Fig. 1), and two upper values $\gamma = 0.63$ and 0.71 , corresponding to the vicinity of the maximum efficiency (see also Fig. 1).

The range of γ from 0.71 to 0.37 examines the propeller wake evolution from a well-constructed wake (corresponding to the maximum efficiency) to a rotor wake affected in its structure by a local flow separation on the blades. It should be emphasized that the choice of parameters γ , in the vicinity of the maximum thrust coefficient τ (see Fig. 1), allows reliable measurement of mean velocities, because there is only a local flow separation upon the blades. For γ lower than 0.2 , complete rotor stalling limits measurement accuracy.

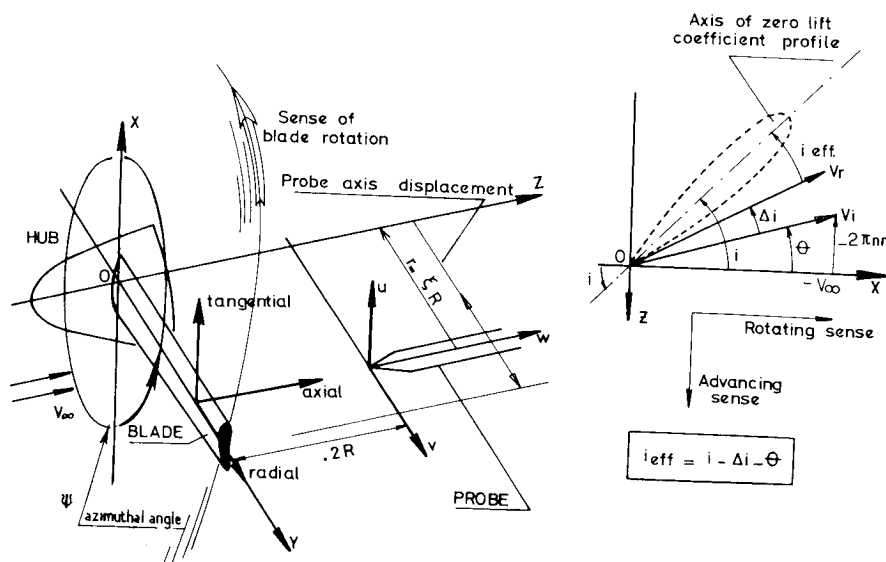
The variations of u , w , v (nondimensionalized by the tangential tip speed $2\pi nR$) with γ , are shown in Figs. 3-5 for values of the reduced blade radius ξ varying from 0.3 to 0.9 . The existence of a point of inflection located between the stalled data ($\gamma = 0.37, 0.45$) and the unstalled data ($\gamma = 0.63, 0.71$) is readily observable on each curve, $\xi = \text{constant}$, of Figs. 3 and 4.

Although the values of u and v remain small in magnitude compared to w , some characteristic quantitative information about the stall mechanism can be obtained from u and v .

Figure 3 shows that for $\xi > 0.6$ and $0.47 < \gamma < 0.63$, the increasing rates of the tangential component u , i.e., $(\partial u / \partial \gamma)$, are slightly larger than those obtained for any other section investigated (except for $\xi = 0.9$, which seems to be influenced by the tip vortex). This phenomenon can be explained by the existence of a flow separation in the region $0.6 < \xi < 0.9$ when $\gamma < 0.63$. In the blade region affected by such a flow separation, the thickening wake of the blade confers rotating motion to a greater mass of fluid in the immediate downstream wake, and thus involves, on the one hand, a slight increase (Fig. 3) in the tangential velocity, and on the other hand, a decrease in the axial velocity (see Fig. 4). In the same way the results plotted in Fig. 5 may describe the flow separation effects on the radial component. Since there is a good correspondence with the results of Fig. 1, as well as those of Figs. 3 and 4, it is worthwhile observing that the sign of the gradient of component v , i.e., $(\partial v / \partial \gamma)$, changes when γ is decreasing in Fig. 5. On the suction side of the blade, the appearance of a bubble due to the flow separation decreases the centrifugal forces on the main flow. This attenuation of the centrifugal effect involves a diminution of the mean radial component of the flow behind the rotor. The regions of negative gradients correspond to an unstalled blade region. So, one can also notice that the profiles obtained for $\gamma = 0.37$ show positive gradients in the region $0.3 < \xi < 0.9$, while for $\gamma = 0.46$ positive gradients are only obtained in the region of $0.6 < \xi < 0.9$. This means that the stalled region first affects the blade tip (although the blade is more heavily loaded at hub than at tip, as can be deduced from the blade pitch angle distribution of Table 1), and then grows from the tip towards the hub with decreasing γ . This last point is in close agreement with similar experimental data already found for the rotating stall in a single-stage axial compressor,⁶ and for the results deduced by a blade oil visualization in Ref. 7.

In order to better evaluate the effects of decreasing γ on the radial component v , it is valuable to draw a parallel with the usual wind-tunnel representation of the lift coefficient vs the incidence of the blade profile. This last representation enables the detection of a stalled flow as soon as the lift coefficient reaches an inversion of the curve slope with the increasing incidences. In Fig. 6 component v is plotted vs the effective incidence $i_{\text{eff}} = i - \Delta i - \theta$, where i denotes the blade pitch angle and Δi is commonly called the induced angle between the directions of incident (V_i) and resultant (V_r) velocities, through the rotor disk (see Fig. 2). As the blade pitch angle law of the propeller was known (see Table 1), the angle Δi as

Fig. 2 Resolution of the vector velocity in the axisymmetric flow.



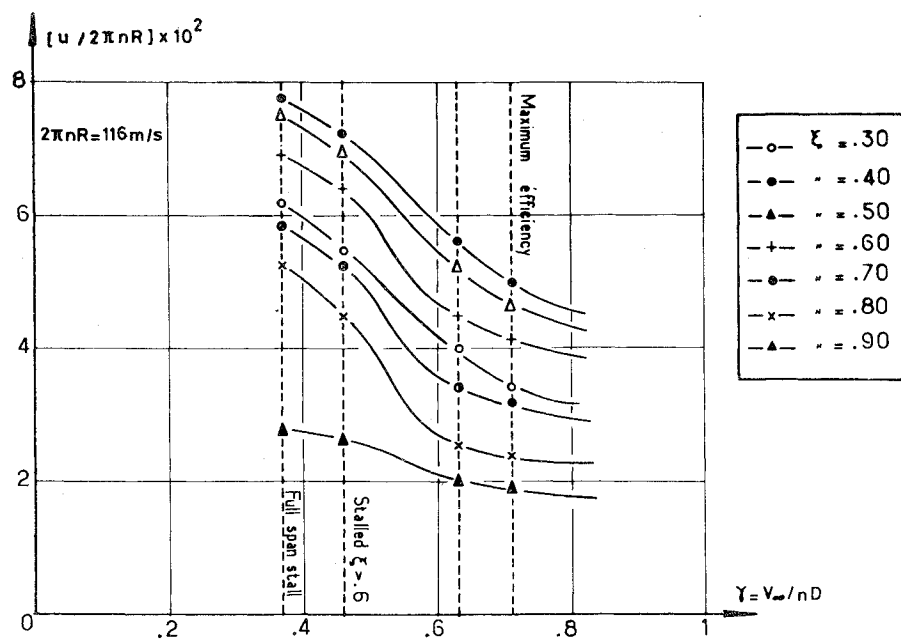
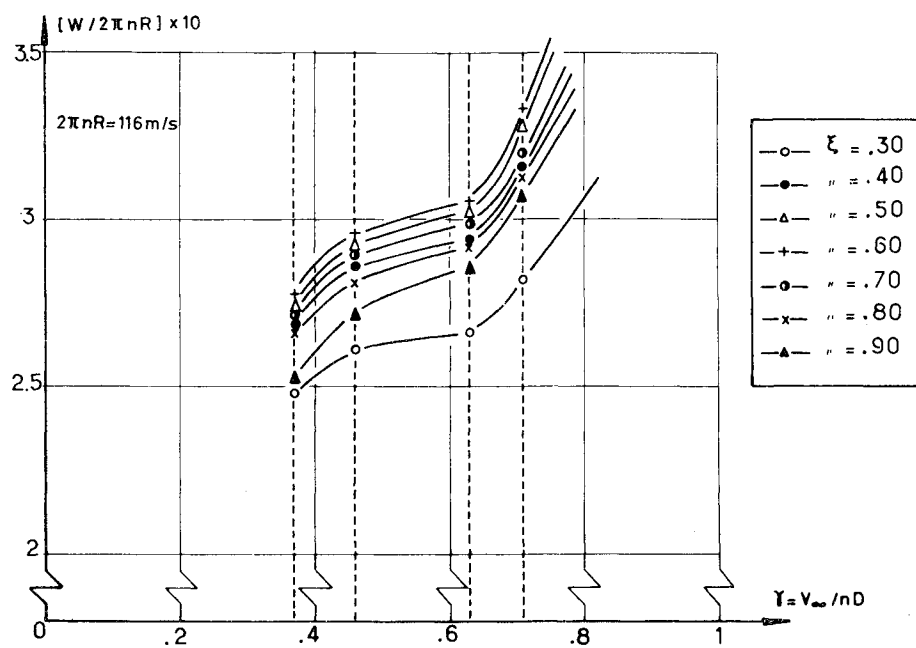
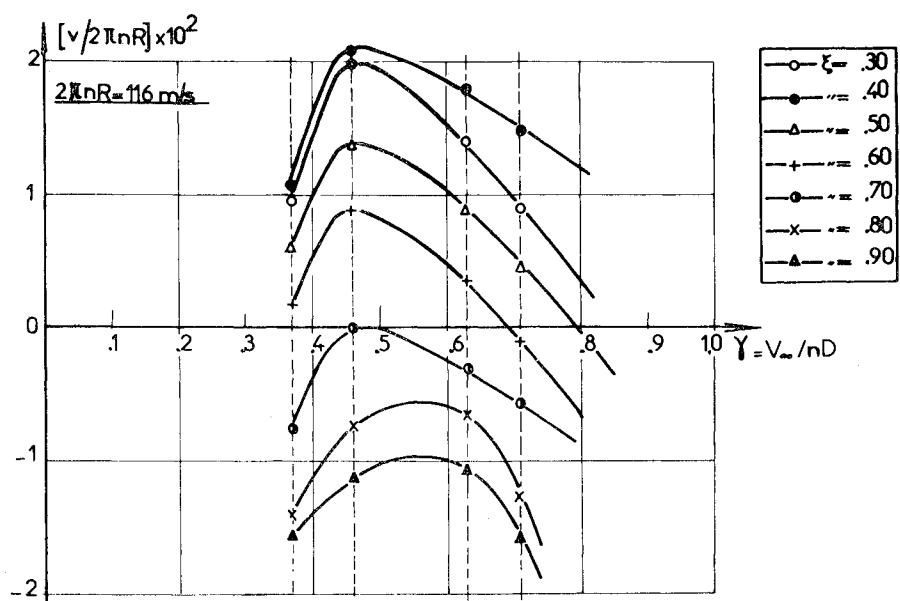
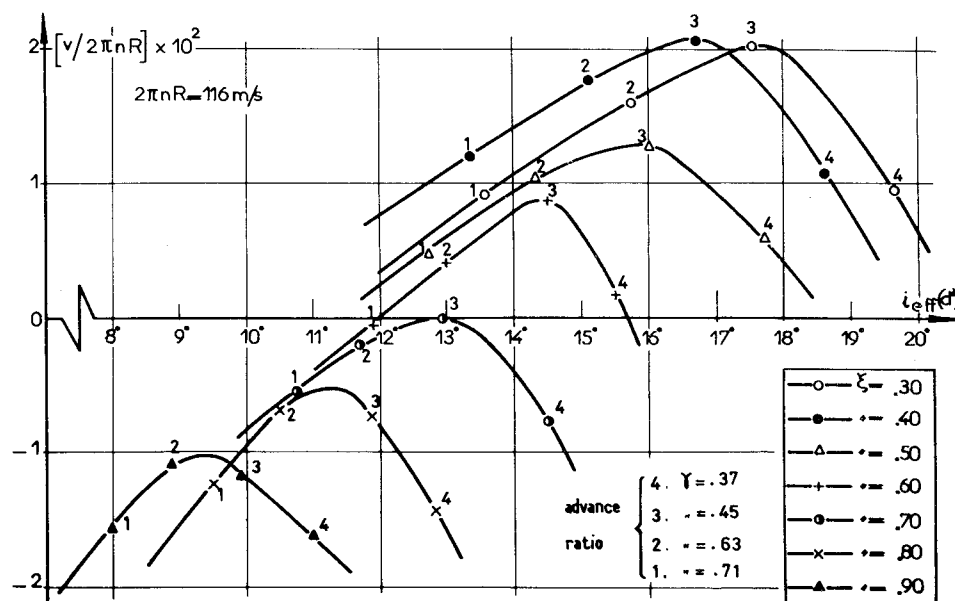
Fig. 3 Evolution of u tangential component vs γ .Fig. 4 Evolution of w axial component vs γ .Fig. 5 Evolution of v radial component vs γ .

Table 1 Geometric propeller data

Reduced radius, $\xi = r/R$	0.176	0.300	0.400	0.500	0.600	0.700	0.800	0.900
Blade chord, l (m)	0.0875	0.124	0.119	0.103	0.086	0.074	0.066	0.061
Relative thickness, e/l	0.187	0.091	0.085	0.082	0.080	0.073	0.051	0.051
Pitch angle, i (deg)	55.1°	48.1°	42.3°	36.3°	31.3°	27°	22.7°	18.6°

Fig. 6 Evolution of v radial component vs the effective incidence i_{eff} .

well as i_{eff} were computed⁴ from the hot-film measurements by using the results obtained on components u and w . In that way, at a given blade section ξ , the curves of Fig. 6 make possible an approximate determination of the stalling incidence related to the sign change of the gradient of each curve. In this figure, it is also of interest to point out that the centrifugal effect tends to delay the stalling incidences which would be reached in a steady flow for the same blade sections. As an example, the stalling incidence of the section $\xi = 0.7$ is already reached⁹ for $i_{\text{eff}} \sim 10^\circ$ in a steady two-dimensional flow, while Fig. 6 gives for $\xi = 0.7$ a stalling incidence near 13° .

This last observation is in good agreement with the results obtained by Himmelskamp⁸ (who used a two-bladed airscrew with a series of Gottigen 625 blade profiles), and lets us think that this kind of representation devoted to plot the radial component vs the effective incidence seems very useful in testing the influence of the blade pitch angle law on the local blade stalling.

Conclusion

From the present investigation it can be concluded that the mean velocity profiles measured in the immediate wake rotor provide insight into the evolution of the wake structure. All the mean components are influenced by the appearance of a local stalling upon the blades. Furthermore, variations in u , v , and w make possible the fine local discrimination of the incidental flow separation, whereas the usual criterion deduced from the variation of the thrust coefficient, $\tau = \tau(\gamma)$, can only provide indication of a global stalling.

In spite of the small values obtained upon the radial velocity, it also appears that the blade pitch angle law can be tested from the variation of this component vs the effective incidences of the blade profiles. One is then led to conclude that these velocity profiles, although primarily of an exploratory nature, can serve as additional data for the construction of a theoretical wake model suited for high thrust levels.

References

- ¹AGARD Congress, CP 102, "Fluid Dynamics of Aircraft Stalling," Lisbon, Portugal, 1972.
- ²AGARD Congress, CP 111, "Aerodynamics of Rotary Wings," Marseille, France, 1972.
- ³Von Mises, R., *Theory of Flight*, McGraw Hill Publications in Aeronautical Sciences, New York, 1945, pp. 319-347.
- ⁴Favier, D., "Contribution a l'etude de l'ecoulement de l'air a l'aval d'une helice a partir de mesures de vitesses au film chaud," These de Specialite, Universite de Provence, Marseille, France, 1973.
- ⁵Favier, D., "Determination des vitesses induites a l'aval d'une helice quadripale a l'aide d'un anemometre a film chaud et a temperature constante," *Compte Rendus de l'Academie des Sciences*, t. 278, A-39, Paris, France, 1974.
- ⁶Valensi, J., "Experimental Investigation of the Rotating Stall in a Single-Stage Axial Compressor," *Journal of Aeronautical Sciences*, Vol. 25, 1958.
- ⁷Prandtl, L., *Guide a travers le Mecanique des Fluides*, Dunod, Paris, France, 1952, pp. 360-361.
- ⁸Schlichting, H., *Boundary Layer Theory*, McGraw-Hill Publication, New York, 1958, pp. 650-651.
- ⁹Abbott, I.A. and Von Doenhoff, A.E., *Theory of Wing Sections*, Dover, New York, 1958, pp. 595-596.